Article

Rule-Based Energy Management System to Enhance PV Self-Consumption in a Building: A Real Case

Haritza Camblong [1,2], Irati Zapirain [1,3], Octavian Curea [3], Juanjo Ugartemendia [4,*], Zina Boussaada [3] and Ramon Zamora [2]

1   Department of Systems Engineering & Control, Faculty of Engineering of Gipuzkoa, University of the Basque Country (UPV/EHU), Europa Plaza 1, E-20018 Donostia, Spain; aritza.camblong@ehu.eus (H.C.); irati.zapirain@ehu.eus (I.Z.)
2   Department of Electrical and Electronic Engineering, Auckland University of Technology, Auckland 1010, New Zealand; ramon.zamora@aut.ac.nz
3   ESTIA Institute of Technology, Technopole Izarbel, University of Bordeaux, 64210 Bidart, France; o.curea@estia.fr (O.C.); z.boussaada@estia.fr (Z.B.)
4   Department of Electrical Engineering, Faculty of Engineering of Gipuzkoa, University of the Basque Country (UPV/EHU), Europa Plaza 1, E-20018 Donostia, Spain
*   Correspondence: juanjo.ugartemendia@ehu.eus

Abstract: The building sector has an important role in the decarbonization of energy. Buildings energy management systems can act on flexible loads to contribute to the integration of renewable energies. This article presents the design, implementation and evaluation of a rule-based energy management systems (RB-EMS) in the frame of a collective self-consumption (CSC) system based on photovoltaic (PV) energy in the Technology Park of Izarbel, in Bidart, France. The RB-EMS acts on the heat ventilation and air conditioning (HVAC) system of one of the buildings involved in the CSC in order to maximize the PV energy self-consumption rate (SCR). Internet of things (IoT) has been developed and implemented in order to retrieve consumption, production and temperature data, and to be able to act on the HVAC. A new 5-step methodology has been developed to design and adjust the RB-EMS. This methodology is mainly based on tests carried out to find the relationship between ON/OFF states of the internal units of the HVAC and the heat pumps' consumption. Finally, the RB-EMS is tested in heating operating mode. The results show that the RB-EMS allows obtaining a SCR of 89%, and that the users comfort limits are respected.

Keywords: collective self-consumption; photovoltaic energy; energy management system; demand side management; flexible loads; heat ventilation and air conditioning (HVAC)

1. Introduction

The International Energy Agency's (IEA) report "Net Zero by 2050. A Roadmap for the Global Energy Sector" [1] puts the timeline for decarbonization compatible with the Paris Agreement in the buildings sector with the next milestones: by 2030, new buildings should be zero-carbon ready and universal energy access facilitated. 2040 is the deadline to retrofit 50% of existing buildings to zero-carbon-ready levels, and by 2050, more than 85% of buildings should be zero-carbon-ready.

On the other hand, the trend towards decentralization and decarbonization of the electricity grid brings with it the importance of the implementation of energy management systems (EMS) in buildings. The implementation of EMSs in buildings can guarantee a significant improvement in their energy efficiency. This fact makes EMSs have a key role in meeting regulatory requirements such as the ones established in European Energy Efficiency Directive (Directive (UE) 2023/1791 [2]), which forces both old and new buildings to obtain a better energy rating.

Furthermore, the point of production is located at the same site as the point of consumption, as well as a storage system or other elements [3–5]. This new grid configuration

trend has been promoted to a certain extent by the technical and legislative development of self-consumption (SC) and of collective self-consumption (CSC). Both concepts were introduced and developed in the French legislative regulation as early as 2016 by means of order nº 2016-1019 of 27 July 2016 relating to self-consumption of electricity [6] and the Article L315-2 of the Energy Code [7], which first introduced the concept of CSC.

In this context, the authors of this article worked on the development and real implementation of such an EMS in the frame of the Interreg V-A Poctefa EKATE project [8]. The global objective of EKATE was to study the "Management of Photovoltaic Electricity and Shared Self-Consumption in the France-Spain cross-border area, using Blockchain technology and the Internet of Things (IoT)". One CSC pilot was developed in the Izarbel technology park. Two articles were published on building consumption and photovoltaic (PV) production forecast models [9,10] as part of a model predictive control EMS type [11] that the authors are developing.

The EMS presented in this article is a rule-based EMS (RB-EMS) and its objective is to maximize the self-consumption rate (SCR) of PV energy actuating on the heating, ventilation and air conditioning (HVAC) of ESTIA2 building involved in the CSC, taking into account the comfort of users.

Several case studies have been found in the literature where EMS has been used to promote self-consumption in buildings. This is the case in [12,13], where the focus is on optimizing the use of PV production in order to reduce the use of the grid as a supplier. In other cases, batteries or electric vehicles (EV) are also managed in order to increase the SCR [14–18] or the overall SCR for an Energy Community [19–22]. Concerning the type of EMS, the most basic EMS are rule-based ones [23–26]. Since RB-EMS is a simple method of control, it is used in a variety of applications. As can be seen in the literature, RB-EMS are widely implemented especially in the e-mobility sector [27,28] and in microgrids [29–31]. RB-EMS is also widely used in buildings but no cases have been found in the literature where it is implemented and evaluated with real tests in the building, although many studies use real data to feed the EMS [5,32].

RB-EMS are also often used in order to increase the SCR of buildings. This is the case in [33], where an EMS is proposed, which combines fuzzy logics with a rule-based algorithm aiming to maximize self-consumption and minimize energy exchange with the grid. As well, in [32], optimization-based and RB-EMS are developed and compared for energy management that consider a PV installation, a battery and the grid itself to supply electricity consumption. The proposed EMS aims to achieve the highest possible SCR, and based on this purpose, it defines six operating modes that depend on how the total consumption can be supplied. The authors conclude that RB-EMS is able to provide more accurate results than optimization-based EMS with less processing time. Similarly, ref. [23] shows a RB-EMS applied to CSC where the rules are individually defined and follow a pattern similar to that of the RB-EMS in [32]. In this case, the rules are simpler. At each time step, the priority is to self-consume the building's energy production. Then, any surplus is used to charge the battery and, finally, it is exported to the grid in case the storage system is full. Import from the grid is the last resort in case of low local production and not enough stored energy inside the battery.

In addition, domestic hot water (DHW) and its associated tank constitute a significant source of consumption in a residential building, with an inertia that can also be used as a flexible load (FL) [34,35]. Among other things, the results of [34] show that it is possible for multi-apartment buildings to provide flexible services by avoiding the use of energy for DHW during peak load hours on the grid. Similarly, in [35] simulations show that about 30% of electricity cost reductions could be obtained with an average comfort fulfilment rate of about 99%. They also show the capability to shift load profile for reducing average power and gross consumption. For example, on a summer day with a demand response (DR) call, a reduction of about 20 kWh of electricity is observed during the demand response period.

Regarding flexible loads (FL) on which EMS can actuate in buildings, one of the main FL used in demand side management (DSM) or demand response is the HVAC

system [36–38]. It is one of the most important FL to consider, with the greatest margin for energy efficiency improvement [39]. The authors of [36] demonstrate the benefits of optimizing the operating costs of heat pumps by achieving 18% cumulative cost savings at the end of the trial period of 2 weeks. In [37], a reduction of 0.9% in terms of total electric consumption is obtained when demand-side flexibility is applied with a further reduction of 0.3% if minimum temperature for occupant comfort is lowered by 1 °C. In [38], two control strategies applied only to the optimization of the HVAC system of an office building are compared. It is concluded that a basic control strategy such as the ON/OFF strategy of the HVAC system can achieve a reduction in consumption of 24.56%.

Associated to the HVAC, the thermal capacity of the building itself is also an important FL to consider. With the methodology used in [40] based on the quantification of 3 performance indicators for the energy flexibility of different building typologies, it is shown that in order to avoid a decrease in storage efficiency, the use of structural thermal energy storage should be limited to short DR events.

Taking into account the existing research studies in the scientific literature, a significant gap between simulated RB-EMS and its real implementation has been observed. Therefore, the main contribution of the work presented in this article is the **design, implementation and critical assessment of an RB-EMS on a real building equipped with a HVAC.** The methodology developed to design the RB-EMS has to be underlined too. In addition, the IoT package developed and installed in the ESTIA2 building and the critical analysis of its operation deserve to be mentioned as a contribution.

The paper is divided into five sections. Section 2 describes the studied CSC case. Section 3 explains how the RB-EMS has been designed. Next, Section 4 shows and analyses the results obtained when applying the developed RB-EMS on ESTIA2 building. Finally, the conclusions related to this research study and some perspectives are given in Section 5.

2. Case Study

2.1. Description of the CSC Case Study and ESTIA2 Building

As shown in Figure 1, the PV energy CSC demonstrator in the Izarbel technology park comprises three buildings: ESTIA1, ESTIA2 and ESTIA4. However, during the period when the work presented in this article was being carried out, the ESTIA1 building was being renovated and communication with the ESTIA1 consumption meters had not been working. For this reason, only ESTIA2 and ESTIA4 buildings were considered in this research study.

Figure 1. The three buildings involved in the CSC of the Izarbel technology park.

The installation of around 60 kWp of *PV* panels is foreseen in these two buildings. As these *PV* panels were not yet installed during the EKATE project, the 5.6 kWp *PV* installed in 2004 in ESTIA1 roof (see Figure 1) were used to emulate the 60 kWp *PV* panels foreseen in ESTIA2 and 4, and thus, to obtain the estimated *PV* power production P_{PV} from Equation (2). For the emulation, the measurement of the electricity produced by the existing panels in ESTIA1, P_{PVB1}, was multiplied by a gain, Equation (1). The gain was calculated by dividing $P_{PVSYSTMAX}$, the maximum power that the new panels would produce according to the PVSyst 8 software [41], i.e., 46.6 kW, by the maximum power produced in 2021 by the current panels, $P_{PVB1MAX}$, i.e., 4.65 kW. The resulting gain, G_{PV}, was approximately 10.

$$G_{PV} = \frac{P_{PV_{SYSTMAX}}}{P_{PV_{B1\ MAX}}} = \frac{46600}{4650} \approx 10 \tag{1}$$

$$P_{PV} = G_{PV} \times P_{PV_{B1}} \tag{2}$$

Regarding the RB-EMS developed in EKATE and presented in this article, it is worth mentioning that it was acting on only one flexible load, the HVAC of ESTIA2 building.

2.2. Developed and Installed IoT in ESTIA2 for the RB-EMS

This sub-section describes the IoT that was used in relation to the RB-EMS. The RB-EMS inputs are the produced PV power, the consumed power in ESTIA2 and 4, the external temperature and the internal temperatures of ESTIA2 rooms. The output variables are the ESTIA2 temperature set-point, same for all rooms, and the ON/OFF state of the HVAC internal master units.

Figure 2 shows the general architecture of this infrastructure. The core of the architecture is a Raspberry Pi processor. It communicates with:

- The Météo France meteorology website;
- The indoor units of the ESTIA2 Daikin HVAC system, via Modbus TCP and a gateway linking to the DIII-net bus;
- The meters of the heat pumps (HP) and the lighting via Ethernet (TCP) and a gateway linking to the KNX bus;
- The cloud and the LoRa network allowing the access to Linky and SME meters data;
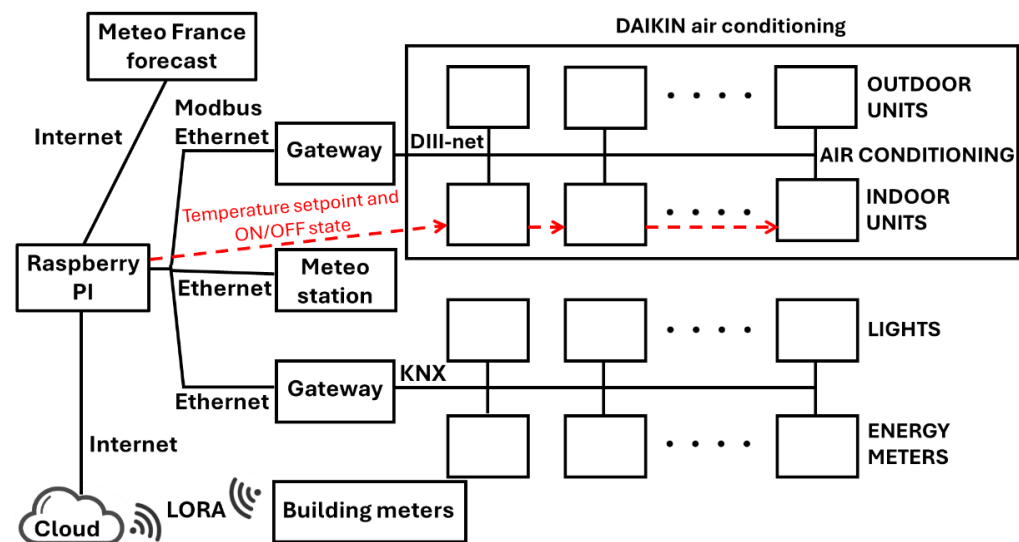- The weather station installed on the ESTIA2 rooftop, via Ethernet.

Figure 2. IoT infrastructure block diagram.

The following subsections present the most important IoT components from the point of view of this research study, focusing on the new devices installed as part of the EKATE project.

2.2.1. Smart Meters and ICT Devices

Meters' data are retrieved thanks to the information and communication technology (ICT) electronic device (see Figure 3) that collects the data specified in Table 1 from the meters and sends them via an antenna using LoRa network. This ICT device was developed by a member of the EKATE consortium. One of the objectives of the EKATE project was to test these ICT devices in the frame of the mentioned CSC energy sharing and the EMS of ESTIA2.
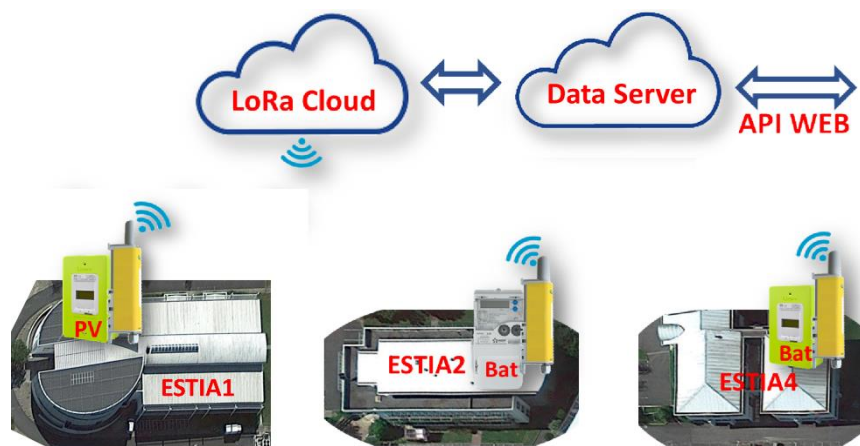

Figure 3. ICT devices connected to the meters in the three building.

Table 1. Meters implicated in the Izarbel CSC.

Building	Meter Type	Measured Magnitude	Data Retrieved	Unit	Sampling Time
ESTIA1	Linky	ESTIA1 PV production	Total injected active energy	Wh	Total injected active energy 10 mn
			Instantaneous injected apparent power	VA	10 mn
ESTIA2	SME/SMI	ESTIA2 consumption	Extracted active energy	kWh	10 mn
			Extracted average active power over 10 min	kW	10 mn
ESTIA4	Linky	ESTIA4 consumption of common parts	Total extracted active energy	Wh	10 mn
			Instantaneous extracted apparent power	VA	10 mn

The ICT devices' antenna enables communication over the LoRa [42] network with the LoRaWAN (Long Range Wide Area Network) protocol. In the context of IoT, it allows structuring a low-power wide area network by integrating low-power terminal equipment through gateways. LoRa is the physical layer that makes it possible to connect sensors or objects that require a very low power or long battery life (counted in years) in a small volume and at low cost. Considering the constraints of the Izarbel CSC pilot, for instance the low power (130 mW) available at smart meter and the need to communicate between different buildings, the abovementioned LoRa characteristics make this network very interesting.

In the Izarbel pilot project, ICT devices retrieve data from smart meters and send it via the LoRa network and the Orange French GSM operator to a data server of a French company. Likewise, the ESTIA2 RB-EMS can retrieve this data through an API.

Table 1 lists some data on the Izarbel meters used by the RB-EMS. The ESTIA1 m that measures the output of the PV panels is of the Linky type [43], as is ESTIA4's consumption meter. The ESTIA2 consumption meter is of the SME/SMI type. It is worth mentioning that ESTIA4, as a business centre, contains several meters. The meter that participates in the CSC measures the consumption of the common areas.

The accessible data and their resolution differ according to the type of meter. The SME/SMI meters provide, among other things, the rate of active energy withdrawn with a resolution of one kWh and the average active power for 10 min in extraction with a resolution of one kW. Linky meters provide the total active energy injected (in production) or withdrawn (in consumption), with a resolution in Wh, and the instantaneous apparent power injected or withdrawn in VA.

Linky meters thus offer much better resolution than SME/SMI meters. The low resolution of SME/SMI meters is a drawback, especially when the consumption of a building equipped with this type of meter is low.

Another problem, observed during the testing of the ICT devices, is the time drift of the time stamped information sent to the data server by the LoRa network. This drift is different from one ICT device to another and does not always occur in the same direction. Thus, it is very difficult to synchronize the data from the different meters. There can be a difference of 5 min between one meter and another. In a 30-min step, corresponding to the time step of the PV production distribution [44], this is not negligible. It was also observed that the data stored on the data server is only available after 20 to 30 min. This is a major handicap for EMS, which requires real-time data. In fact, the data server platform and the communication via the mentioned commercialized ICT devices and LoRa were designed for monitoring PV plants.

2.2.2. ESTIA2 HVAC System

The ESTIA2 HVAC system consists of 10 outdoor HP units and 73 indoor units composed of a vent and boxes/thermostats, as shown in Figure 4. Of the 73 indoor units, 60 are master units. All these units are Daikin branded. ESTIA2 has 4 flours and 68 rooms. Some rooms have more than one internal unit, and each external unit is linked to 5 to 8 internal units (see Appendix A).

Figure 4. External and internal units of the ESTIA2 HVAC system.

The gateway that links the Modbus and the Daikin DIII network (see Figure 2) allows data such as the temperature of each room to be retrieved. The gateway also allows adjusting the set-point temperatures for each office or room as well as the ON/OFF status of the internal master units.

Another gateway is used to link to the KNX bus to recover the energy consumption of the external units (Figure 2). In fact, as part of the project, an electricity meter was installed in each external group. The consumption of these groups is the main consumption of the building.

3. Rule-Based Energy Management System Design and Assessment Methodology

A new methodology was established to design and assess the RB-EMS. The objective of the methodology was to design an RB-EMS that has the objectives mentioned in Section 1

and the inputs and outputs mentioned in Section 2, and that is valid for every building with a HVAC based on HP and whose main power consumption is linked to the HVAC operation. The steps of the methodology are presented in Figure 5.
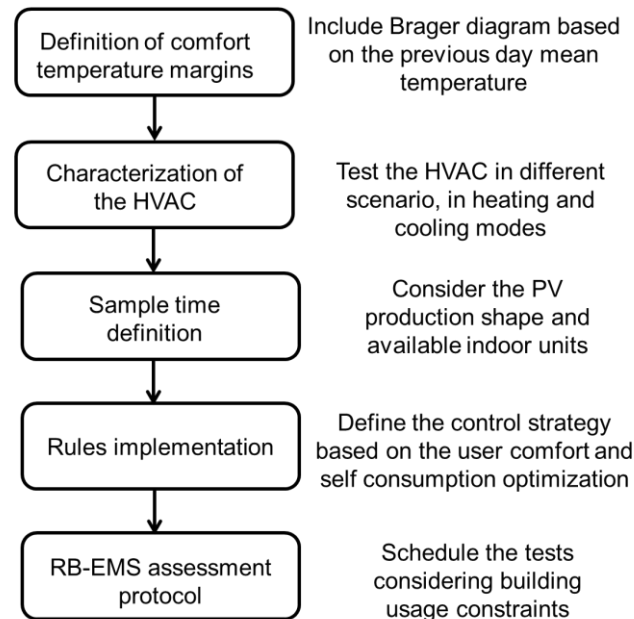

Figure 5. Steps of the developed methodology to design the RB-EMS.

3.1. Method for the Definition of Comfort Temperature Margins

The comfort temperature margins definition is based on the Brager diagram [45]. Figure 6 illustrates this diagram. The average external temperature is represented on the *x*-axis.
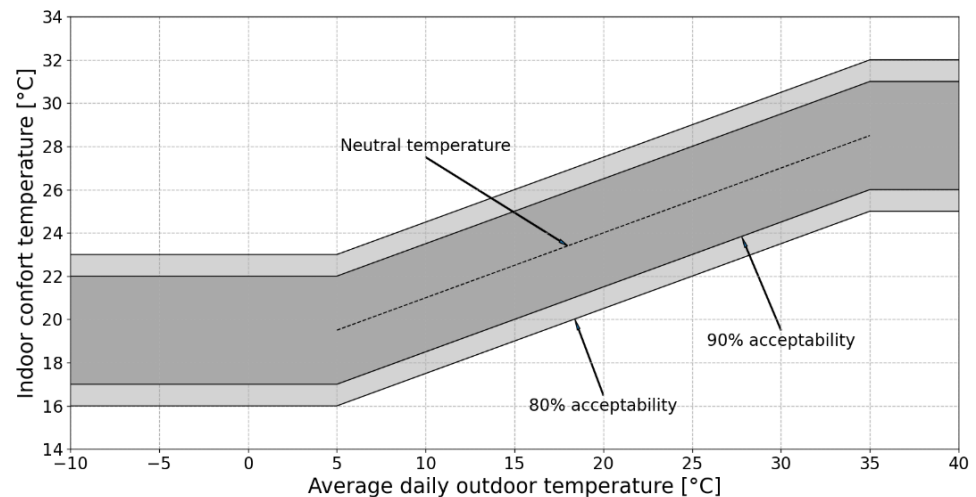

Figure 6. Definition of comfort temperature margins based on Brager diagram.

As shown in Figure 6, the 90% acceptability interval around the neutral temperature T_n has a width of 5° (between $T_{min\_90\%}$ and $T_{max\_90\%}$), while this width is 7° for the 80% acceptability interval (between $T_{min\_80\%}$ and $T_{max\_80\%}$). The margins of this diagram could be changed, for example depending on the usual humidity of the place. It can also be used to prioritize the SCR, the comfort or the building efficiency, adjusting the temperatures limits of the acceptable comfort zone, T_{min} and T_{max}.

3.2. Carrying out Tests for the Characterization of the HVAC

HVAC characterization tests are necessary to know the influence on the building's consumption of the units turned on. As an example, Figure 7 shows the results obtained during one of these tests where five internal units of external group 3 were switched ON consecutively. The units 1 to 5, located in different rooms, are linked to the same external group. The related temperatures are shown with different colours. These temperatures are displayed as zero when the units are OFF. In all cases, the set-point temperature is 21 °C. The units operate in cooling mode. Figure 8 shows the evolution of the third external group HP power consumption in the same test.
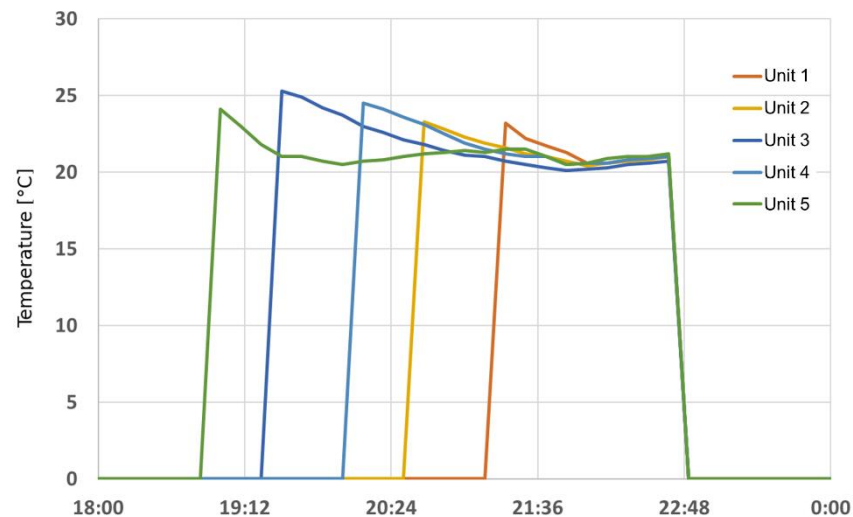

Figure 7. Internal temperature obtained during one test applied to 5 internal units related to external group 3.
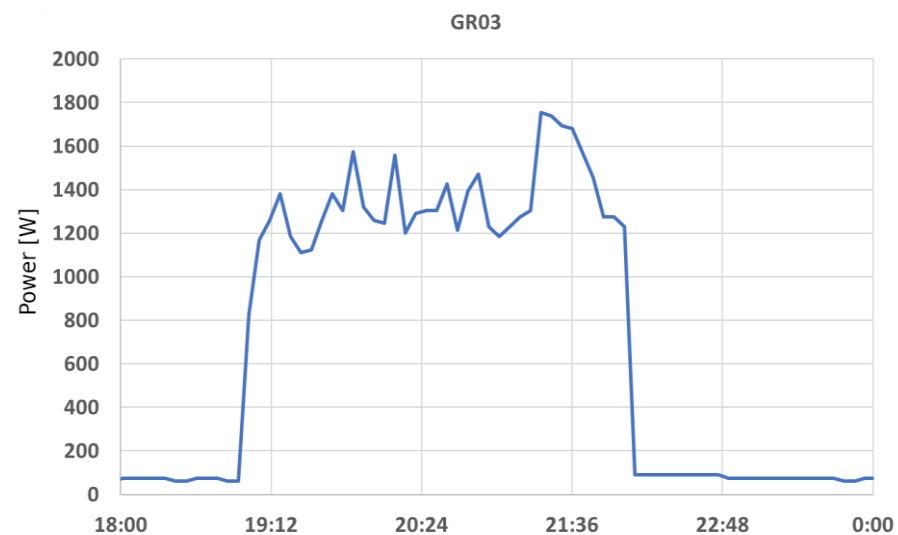

Figure 8. Power consumption of the third external group HP.

The main conclusions of the carried-out tests are the following:

- After the first indoor unit associated to an external group is switched ON, when new indoor units associated with the same group are switched ON, the variation of the power consumption is not very significant.
- When an external unit is switched ON through the solicitation of an internal unit, a significant consumption power step is produced. This step is of 2 kW in average (around 1.4 kW for group 3 in Figure 8) when the difference between the set-point and

rooms indoor temperatures are lower than 5°, while ensuring that comfort criteria are always respected.

- When an internal unit is switched ON, the temperature overpassing is lower than one degree.

3.3. RB-EMS Sample Time Definition

In order to have the best consumption power steps/variations resolution, it is important to be able to act on all outdoor groups and indoor master units in one day. In our case, there are 60 indoor master units, and it takes five hours to reach the typical PV production bell in the absence of cloud. Therefore, a sampling time of five minutes would allow switching ON all the master units one by one up to the mentioned bell.

3.4. RB-EMS Rules

As explained before, the goal of the RB-EMS is to increase the self-consumption rate, taking into account the comfort of the users.

During the night, when there is no PV production, the indoor units are managed in order to obtain the minimum comfort temperature ($T_{min\_90\%}$) at the beginning of the workday. It is necessary to ensure the comfort even if this procedure increases non-renewable energy consumption.

Figure 9 shows the flow-chart related to the RB-EMS for the case where the HP works in heating mode (HM). P_C is the average power consumed in ESTIA 2 and 4. The parameter $h = 2$ kW is the hysteresis threshold of the PV surplus power used to decide if new indoor units should be switched ON or switched OFF.
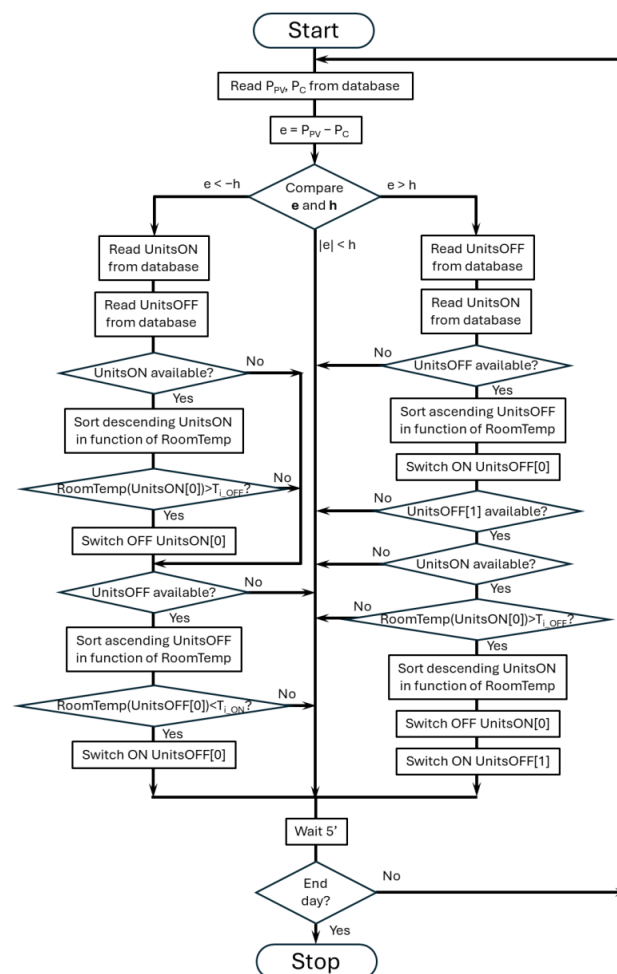

Figure 9. Flow-chart that depicts the rules of the RB-EMS2 for HM.

The units that must be prioritized to be switched ON are the ones with the lowest temperature and close to the comfort limits, while the highest temperature for units that must be switched OFF. In addition, supplementary units are switched ON and OFF in order to homogenize temperatures as much as possible. Three cases are considered:

- If enough PV surplus is available ($e > h$), then the OFF unit (*UnitsOFF*) with the lowest temperature is switched ON (*UnitsOFF*[0] after ascending sort). Then, if the temperature of the ON unit related to the highest temperature is higher than T_{i_OFF}, it is switched OFF and the next OFF unit related to the lower temperature (*UnitsOFF*[1]) is switched ON.
- If $-h < e < h$, no unit is switched ON or OFF.
- If $e < -h$, then the ON unit related to the highest temperature (if higher than T_{i_OFF}) is switched OFF and the remaining OFF unit related to the lower temperature (if lower than that T_{min}) is switched ON. In this case. the priority is given to the comfort, even if the energy is consumed from the grid.
- In order to consider the thermal dynamics of the rooms, T_{i_ON} and T_{i_OFF} are set to $T_{min\_90\%} + 1°$ and $T_n - 1°$, respectively. Even after switching OFF an internal unit, the temperature increases for a while. If the limit for switching ON was set to $T_{min\_90\%}$, in some situations the room temperature could decrease under this value, so going out of the comfort interval.

3.5. RB-EMS Assessment Protocol

As in this study case, it is common to not be able to carry out assessment tests under normal building occupancy conditions. For these cases, the following assessment protocol is designed:

1. The test is performed on a day where the building is empty, for instance on a Sunday as here;
2. The obtained SCR with the RB-EMS is compared with the estimation of the SCR that would be obtained in the same day without the RB-EMS.

The *SCR* is calculated as follows [12]:

$$SCR = \frac{\sum E_{PV}^{cons}}{\sum E_{PV}^{prod}} \tag{3}$$

where E_{PV}^{cons} represents the *PV* energy consumed and E_{PV}^{prod} represents the *PV* energy produced, both in one self-consumption period (30 min in France).

4. Results and Discussion

This section presents the results obtained in a real test carried out in HM. The test was carried out on a Sunday, as mentioned in the previous section.

The mean external temperature applied to the Brager diagram was 4.2 °C and the priority was given to the comfort, considering a 90% comfort zone (between 17 and 22 °C). Taking into account the hysteresis and dynamics of the HVAC and building, T_{min} was adjusted as follows: $T_{min} = T_{min\_90\%} + 1$.

Figure 10 shows the production and consumption curves for this day. The PV production curves is drawn in blue. The curve in orange represents the consumption of buildings 2 and 4. The self-consumed energy is drawn in red and the consumption of the HP (the flexible load) in purple. All quantities represent the energy produced or consumed during 30 min time interval (the interval related to the calculation of the PV energy sharing in France [44] in kWh).

The consequences of the delay of 20 to 30 min in recovering power data from the data server described in Section 2.2.1. can be observed in Figure 10. There is a delay between the PV production and the HP consumption (and as a consequence of the building's consumption). This lag is mainly seen when there is a relatively abrupt change in PV production. For example, it can easily be observed between 12:30 and 13:30. Despite this

delay, the effect of the RB-EMS on self-consumption is remarkable. The total consumption curve follows that of the PV production well. The obtained average SCR is 89%.
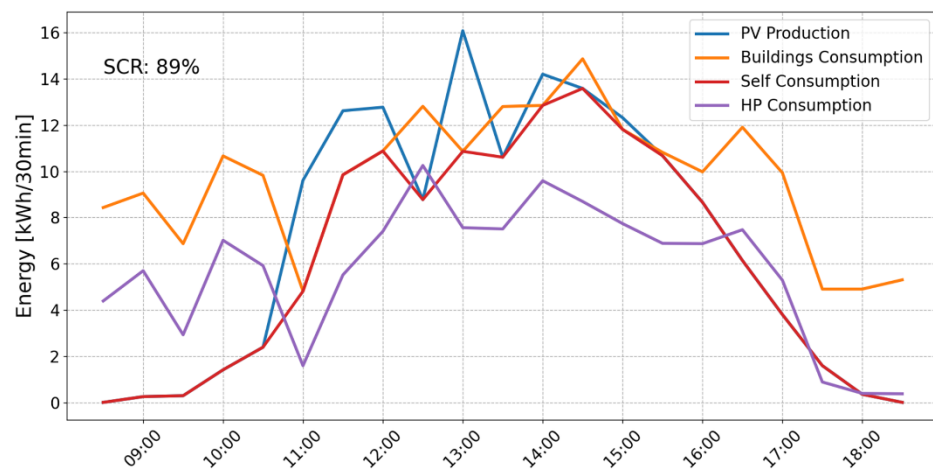

Figure 10. Self-consumption analysis in the HM test with RB-EMS.

Figure 11 depicts the evolution of the number of indoor units switched on. It can be seen that this trend is linked to the HP consumption profile. Comparing with the production curve, again, a delay is observed.
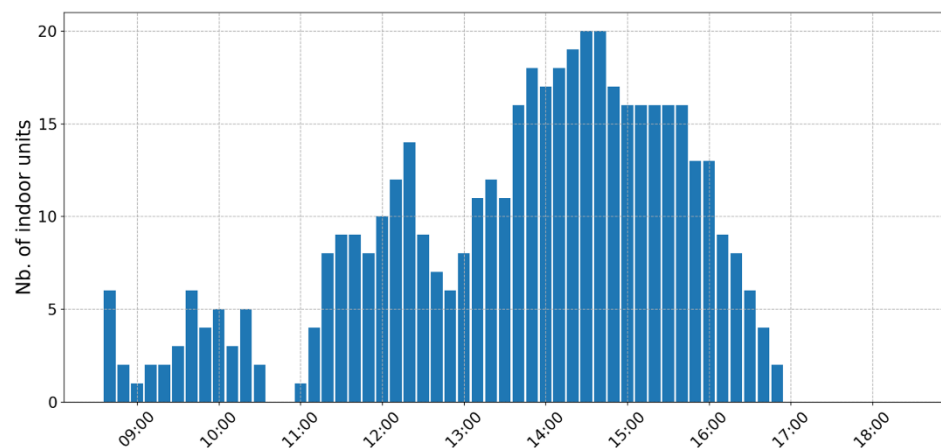

Figure 11. Evolution of the number of indoor units switched ON.

Figure 12 shows the average temperature of the four levels of ESTIA2. The comfort zone limits are respected in general, except in the floor 4 in the afternoon. The effect of the sun leads to the comfort limit being exceeded. As the HP work in HM, they cannot reduce this temperature.

It is also worth mentioning that the lower comfort limit given by Brager diagram is very low (17 °C). The diagram should be adjusted to avoid this situation. Because of the mentioned low limit, the temperature of level 1 (one part underground) is very low at the beginning of the morning and at the end of the afternoon. Anyway, the temperature is always within the fixed comfort limits during these times of the day. Moreover, it can be observed that this temperature varies significantly. It is because only three of the six rooms on this floor are equipped with indoor units.

Figure 13 depicts the estimation of the self-consumption that would be obtained in the same day if the RB-EMS was not operating. The SCR obtained would be only 48%. This value agrees with values found in literature [25]. The estimation of the consumption is based on the consumption of the building on Sundays (very similar on all Sundays). The obtained SCR is much lower, but of course, the comparison has its limits. Indeed, if the

test without the RB-EMS had been carried out on a weekday, the consumption would have naturally increased in the morning and decreased in the afternoon [9].
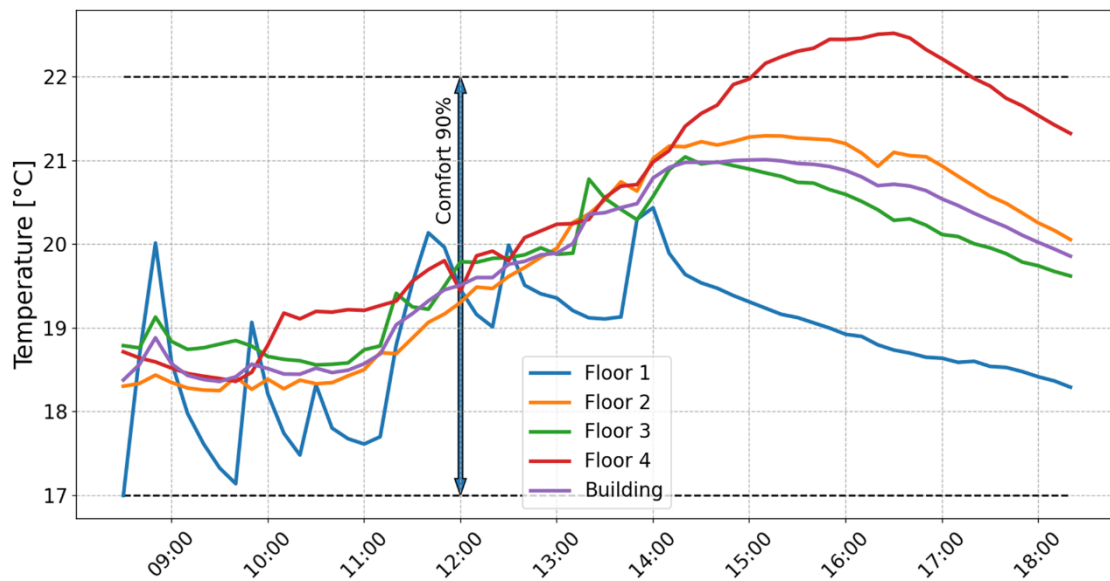

Figure 12. Four levels temperatures and the comfort level in the HM test.
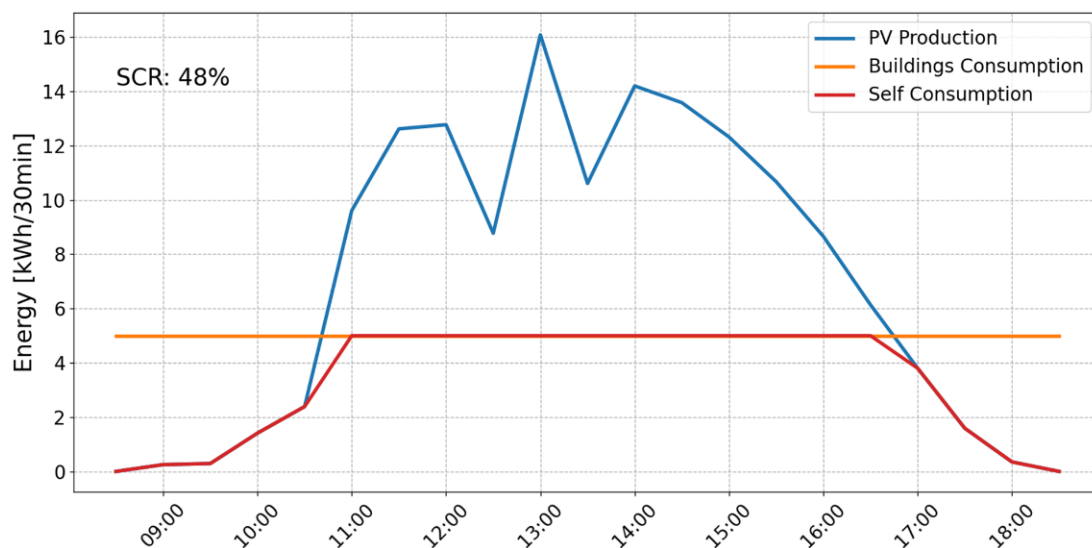

Figure 13. SCR estimated for the case without the RB-EMS during the day-day.

The obtained results show that with a simple RB-EMS, PV energy self-consumption can be improved, using FL instead of introducing batteries, as proposed in other works [25].

The real tests have been carried out for only one day. More scenarios and cases should be considered to obtain a more general conclusion about the improvement of the self-consumption with the developed RB-EMS, and about the consideration of the comfort levels. Therefore, as here, more tests should be done on Sundays. However, the challenge would be to perform real tests in working days when HP are really used to heat (in winter) or cool (in summer) the building. For that, different steps should be first completed in order to ensure the reliability of the EMS in general, and especially of the ICT part. This would allow experiments to be carried out without disrupting the work of the building's users.

Another solution to generalize this research study could be to simulate the RB-EMS using historical production and consumption data. However, the HVAC system of ESTIA2 is very complex to model, due mainly to its decentralized structure and old age (20 years).

Therefore, as experienced by this research study team, it is nearly impossible to develop a highly reliable simulation model of the system.

The above discussions explain some of the reasons why our team has not found any publication on the implementation and experimentation of RB-EMS for energy SC in real buildings.

5. Conclusions

The research study presented in this article analyses the management of the consumed energy in ESTIA2 building by acting on the HVAC. The objective was to maximize the SCR respecting the building users temperature comfort limits. Thus, a RB-EMS and the associated ICT were developed, implemented and tested in the real system.

The results of the test demonstrate the efficiency of the developed RB-EMS. The EMS allows following the PV production curves while respecting the defined comfort limits. On the HM test, the SCR obtained with the RB-EMS is 89% while that obtained without the EMS is 48%. This means that the RB-EMS delivers an 85% improvement over the case without EMS. Of course, as above mentioned, this comparison has some limits, but it is the first assessment step. In the next step, the comparison protocol will have to be improved to generalize the research study.

Regarding the developed methodology, it is valid for every building with a HVAC based on HP and whose main power consumption is linked to the HVAC operation. Once the research study is generalised, the methodology will become a good guideline for energy system designers and managers planning to implement this kind of EMS.

Another important conclusion of the study is that the ICT used to manage production and consumption data had a lack of precision and reliability that affected negatively the performance of the developed RB-EMS. One of the main problems is the time delay occurred in the process between measurements and downloading data from the cloud. A local management of data would be a good alternative to face this problem.

Concerning future works, considering the impact of ICT problems met when retrieving production and consumption data, the first task will be to create and implement a local LoRa network associated to a local server in Izarbel. Then, once ensured that this local communication infrastructure works well, with the authorization of the Management of ESTIA, the RB-EMS will be tested in different scenario, especially on weekdays. Finally, an optimized EMS based on the model predictive control technique is being developed and will be implemented and tested in ESTIA2. Thus, the two EMS will be compared on the real system.

Appendix A Characteristics of HVAC

Table A1 gives some characteristics of the external groups. It can be noted that there are different product ranges. Some units are more powerful than others are, and they have two compressors. The number of internal units that can be connected to each unit is also different depending on the range.

It can be observed that the COP (coefficient of performance) of all the units is between 3 and 4, both in heating and cooling mode. As for the nominal power of the units, it varies between 4.34 kW for the least powerful units and 10.8 kW for the most powerful units.

Table A1. Characteristics of external groups.

Group	Range	Nominal Capacity (kW)		COP		Power Input (kW)	
		Cooling	Heating	Cooling	Heating	Cooling	Heating
1	RXYQ5M7W1B	14	16	3.69	3.69	3.79	4.34
2	RXYQ8M7W1B	22.4	25	3.21	3.63	6.97	6.89
3	RXYQ12M7W1B	33.5	37.5	3.16	3.47	10.6	10.8
4	RXYQ8M7W1B	22.4	25	3.21	3.63	6.97	6.89
5	RXYQ12M7W1B	33.5	37.5	3.16	3.47	10.6	10.8
8	RXYQ5M7W1B	14	16	3.69	3.69	3.79	4.34
9	RXYQ5M7W1B	14	16	3.69	3.69	3.79	4.34
10	REYQ10M7W1B	28	31.5	3.11	3.38	9	9.31
11	REYQ12M7W1B	33.5	37.5	3.16	3.47	10.6	10.8
16	REYQ10M7W1B	28	31.5	3.11	3.38	9	9.31

Table A2 shows data on the relationship between internal and external units. It can be seen that the maximum number of internal units per external unit varies from 8 to 20. In addition, as mentioned above, the number of compressors varies from one to two depending on the range of the outdoor unit. For example, unit 16 has two compressors. One operates in ON/OFF and the other in modulation.

Table A2. Other characteristics of external groups.

Group	Range	Connectable Indoor Units	Number of Compressors	Total Capacity of Connectable Indoor Units (kW)
1	RXYQ5M7W1B	8	1	[7; 18.2]
2	RXYQ8M7W1B	13	2	[11.2; 29.1]
3	RXYQ12M7W1B	19–20	2	[16.8; 43.6]
4	RXYQ8M7W1B	13	2	[11.2; 29.1]
5	RXYQ12M7W1B	19–20	2	[16.8; 43.6]
8	RXYQ5M7W1B	8	1	[7; 18.2]
9	RXYQ5M7W1B	8	1	[7; 18.2]
10	REYQ10M7W1B	16	2	
11	REYQ12M7W1B	19–20	2	
16	REYQ10M7W1B	16	2	

Graphical interfaces have been designed to make it easier to observe the main variables of the internal units, making the interpretation of the tests easier. Figure A1 shows the graphical interface designed for the internal units on the ground floor. It can be seen that some rooms have more than one internal unit. Each room is numbered. The symbols corresponding to the internal units are framed in red or blue. When the inside of the frame is coloured, the unit is switched ON. A blue frame means that the unit is configured in cooling mode, while a red frame means that it is in heating mode. The number inside the circle represents the internal temperature measured by the unit's sensor. One unit only works in cooling mode because room 16 must always be cooled. This explains the fact that in room 19 one unit is configured in cooling mode and the other in heating mode. Indeed, as the unit of room 16 and the L1.200 unit (Daikin DIII-net address) in room 19 belong to the same external group, the L1.200 unit also operates in cooling mode. As room 19 contains another indoor unit, the L1.200 unit can be kept OFF during the cold season.
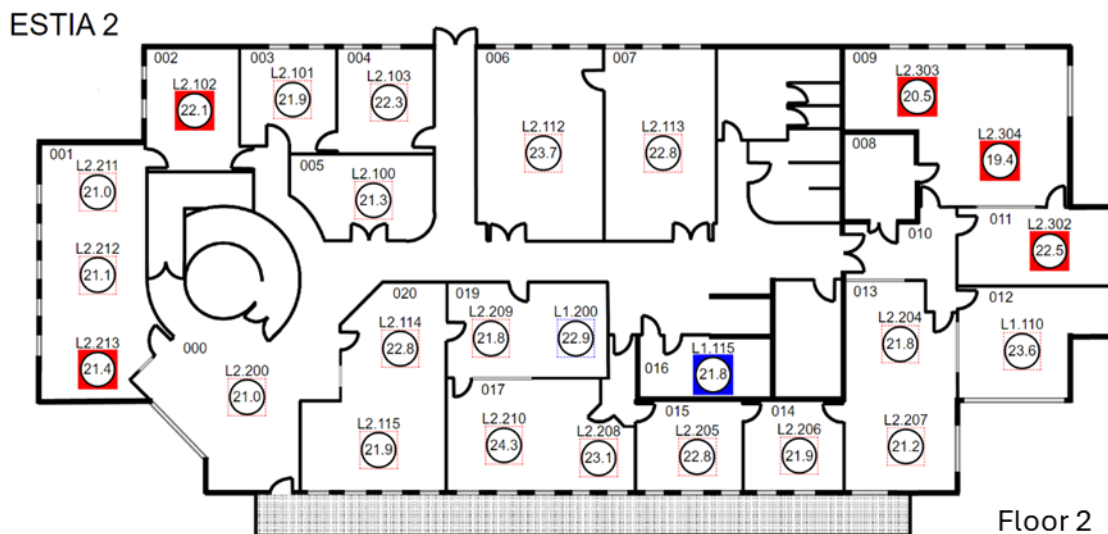
Figure A1. Graphic interface of the internal units on the ground floor (red: heating, blue: cooling).

References

1. Net Zero by 2050—Analysis'. IEA. Available online: https://www.iea.org/reports/net-zero-by-2050 (accessed on 11 July 2023).
2. European Parliament; Council of the European Union. Directive (EU) 2023/1791 of 13 September 2023 on Energy Efficiency and Amending Regulation (EU) 2023/955 (Recast). Official Journal of the European Union. 20 September 2023. Available online: https://eur-lex.europa.eu/eli/dir/2023/1791/oj (accessed on 24 May 2024).
3. Bosu, I.; Mahmoud, H.; Ookawara, S.; Hassan, H. Applied single and hybrid solar energy techniques for building energy con-sumption and thermal comfort: A comprehensive review. *Sol. Energy* **2023**, *259*, 188–228. [CrossRef]
4. Maask, V.; Rosin, A.; Roasto, I. Development of Experimental Load Management System for Nearly Zero-Energy Building. In Proceedings of the 2018 IEEE 59th International Scientific Conference on Power and Electrical Engineering of Riga Technical University (RTUCON), Riga, Latvia, 12–13 November 2018; pp. 1–5.
5. Rafique, S.; Hossain, M.J.; Nizami, M.S.H.; Bin Irshad, U.; Mukhopadhyay, S.C. Energy Management Systems for Residential Buildings With Electric Vehicles and Distributed Energy Resources. *IEEE Access* **2021**, *9*, 46997–47007. [CrossRef]
6. Ministère de L'environnement; De L'énergie et de la Mer. Ordonnance no 2016-1019 du 27 Juillet 2016 Relative à L'autoconsommation D'électricité'. Journal Officiel de la République Francaise. 28 July 2016. Available online: https://www.legifrance.gouv.fr/loda/id/JORFTEXT000032938257 (accessed on 14 November 2024).
7. Légifrance. Code de L'énergie. *Chapter V: Self-Consumption (Article L315-1 to L315-8).* Available online: https://www.legifrance.gouv.fr/codes/article_lc/LEGIARTI000043213495 (accessed on 1 July 2021).
8. Interreg POCTEFA (Spain—France—Andorra) ● Interreg.eu, Interreg.eu. Available online: https://interreg.eu/programme/interreg-spain-france-andorra/ (accessed on 1 December 2022).
9. Zapirain, I.; Etxegarai, G.; Hernández, J.; Boussaada, Z.; Aginako, N.; Camblong, H. Short-term electricity consumption forecasting with NARX, LSTM, and SVR for a single building: Small data set approach. *Energy Sources Part A Recover. Util. Environ. Eff.* **2022**, *44*, 6898–6908. [CrossRef]
10. Etxegarai, G.; Zapirain, I.; Camblong, H.; Ugartemendia, J.; Hernandez, J.; Curea, O. Photovoltaic Energy Production Forecasting in a Short Term Horizon: Comparison between Analytical and Machine Learning Models. *Appl. Sci.* **2022**, *12*, 12171. [CrossRef]
11. Boralessa, M.A.K.S.; Hovden, S.; Wickramarathna, A.V.U.A.; Hemapala, K.T.M.U. Effect of Renewable Energy Forecasting Error on Model Predictive Control Based Microgrid Energy Management System. In Proceedings of the 2022 IEEE IAS Global Conference on Emerging Technologies (GlobConET), Arad, Romania, 20–22 May 2022; pp. 959–962.
12. Tercan, S.M.; Demirci, A.; Gokalp, E.; Cali, U. Maximizing self-consumption rates and power quality towards two-stage evaluation for solar energy and shared energy storage empowered microgrids. *J. Energy Storage* **2022**, *51*, 104561. [CrossRef]
13. Ettalbi, K.; Elabd, H.; Ouassaid, M.; Maaroufi, M. A Comparative Study of Energy Management Systems for PV Self-Consumption. In Proceedings of the 2016 International Renewable & Sustainable Energy Conference (Irsec' 16), Marrakech, Morocco, 14–17 November 2016; Essaaidi, M., Zaz, Y., Eds.; IEEE: New York, NY, USA, 2016; pp. 1086–1091. Available online: https://www.webofscience.com/wos/woscc/full-record/WOS:000466883000201 (accessed on 13 July 2023).
14. van der Meer, D.; Mouli, G.R.C.; Mouli, G.M.-E.; Elizondo, L.R.; Bauer, P. Energy Management System With PV Power Forecast to Optimally Charge EVs at the Workplace. *IEEE Trans. Ind. Inform.* **2016**, *14*, 311–320. [CrossRef]
15. Sorour, A.; Fazeli, M.; Monfared, M.; Fahmy, A.; Searle, J.; Lewis, R. Enhancing Self-consumption of PV-battery Systems Using a Predictive Rule-based Energy Management. In Proceedings of the 2021 IEEE PES Innovative Smart Grid Technologies Europe (ISGT Europe), Espoo, Finland, 18–21 October 2021; pp. 1–6.

16. Salpakari, J.; Rasku, T.; Lindgren, J.; Lund, P.D. Flexibility of electric vehicles and space heating in net zero energy houses: An optimal control model with thermal dynamics and battery degradation. *Appl. Energy* **2017**, *190*, 800–812. [CrossRef]

17. Toosi, H.E.; Merabet, A.; Swingler, A.; Al-Durra, A. Optimal battery cycling strategies in workplaces with electric vehicle chargers, energy storage systems and renewable energy generation. *IET Renew. Power Gener.* **2022**, *16*, 1121–1133. [CrossRef]

18. Gudmunds, D.; Nyholm, E.; Taljegard, M.; Odenberger, M. Self-consumption and self-sufficiency for household solar producers when introducing an electric vehicle. *Renew. Energy* **2020**, *148*, 1200–1215. [CrossRef]

19. Al-Sorour, A.; Fazeli, M.; Monfared, M.; Fahmy, A.; Searle, J.R.; Lewis, R.P. Enhancing PV Self-Consumption Within an Energy Community Using MILP-Based P2P Trading. *IEEE Access* **2022**, *10*, 93760–93772. [CrossRef]

20. Aranzabal, I.; Gomez-Cornejo, J.; López, I.; Zubiria, A.; Mazón, J.; Feijoo-Arostegui, A.; Gaztañaga, H. Optimal Management of an Energy Community with PV and Battery-Energy-Storage Systems. *Energies* **2023**, *16*, 789. [CrossRef]

21. Barone, G.; Brusco, G.; Menniti, D.; Pinnarelli, A.; Polizzi, G.; Sorrentino, N.; Vizza, P.; Burgio, A. How Smart Metering and Smart Charging may Help a Local Energy Community in Collective Self-Consumption in Presence of Electric Vehicles. *Energies* **2020**, *13*, 4163. [CrossRef]

22. Surmann, A.; Walia, R.; Kohrs, R. Agent-based bidirectional charging algorithms for battery electric vehicles in renewable energy communities. *Energy Inform.* **2020**, *3*, 1–12. [CrossRef]

23. Mustika, A.D.; Rigo-Mariani, R.; Debusschere, V.; Pachurka, A. A two-stage management strategy for the optimal operation and billing in an energy community with collective self-consumption. *Appl. Energy* **2022**, *310*, 118484. [CrossRef]

24. Chakraborty, S.; Modi, G.; Singh, B. A Cost Optimized-Reliable-Resilient-Realtime- Rule-Based Energy Management Scheme for a SPV-BES-Based Microgrid for Smart Building Applications. *IEEE Trans. Smart Grid* **2022**, *14*, 2572–2581. [CrossRef]

25. Li, H.; Zhang, H.; Zou, B.; Peng, J. A generalized study of photovoltaic driven air conditioning potential in cooling season in mainland China. *Renew. Energy* **2024**, *223*, 120048. [CrossRef]

26. Chabaud, A.; Eynard, J.; Grieu, S. A rule-based strategy to the predictive management of a grid-connected residential building in southern France. *Sustain. Cities Soc.* **2017**, *30*, 18–36. [CrossRef]

27. Kang, J.; Guo, Y.; Liu, J. Rule-based Energy Management Strategies for a Fuel Cell-Battery Hybrid Locomotive. In Proceedings of the 2020 IEEE 4th Conference on Energy Internet and Energy System Integration (EI2), Wuhan, China, 30 October–1 November 2020; pp. 45–50.

28. Zhou, S.; Chen, Z.; Huang, D.; Lin, T. Model Prediction and Rule Based Energy Management Strategy for a Plug-in Hybrid Electric Vehicle With Hybrid Energy Storage System. *IEEE Trans. Power Electron.* **2020**, *36*, 5926–5940. [CrossRef]

29. Jafari, M.; Malekjamshidi, Z. Optimal energy management of a residential-based hybrid renewable energy system using rule-based real-time control and 2D dynamic programming optimization method. *Renew. Energy* **2019**, *146*, 254–266. [CrossRef]

30. Ouédraogo, S.; Faggianelli, G.; Notton, G.; Duchaud, J.; Voyant, C. Impact of electricity tariffs and energy management strategies on PV/Battery microgrid performances. *Renew. Energy* **2022**, *199*, 816–825. [CrossRef]

31. Torres-Moreno, J.L.; Gimenez-Fernandez, A.; Perez-Garcia, M.; Rodriguez, F. Energy Management Strategy for Micro-Grids with PV-Battery Systems and Electric Vehicles. *Energies* **2018**, *11*, 522. [CrossRef]

32. Herath, A.; Kodituwakku, S.; Dasanayake, D.; Binduhewa, P.; Ekanayake, J.; Samarakoon, K. Comparison of Optimization- and Rule-Based EMS for Domestic PV-Battery Installation with Time-Varying Local SoC Limits. *J. Electr. Comput. Eng.* **2019**, *2019*, 8162475. [CrossRef]

33. Sorour, A.; Fazeli, M.; Monfared, M.; A Fahmy, A.; Searle, J.R.; Lewis, R.P. Forecast-Based Energy Management for Domestic PV-Battery Systems: A U.K. Case Study. *IEEE Access* **2021**, *9*, 58953–58965. [CrossRef]

34. Sørensen, L.; Walnum, H.T.; Sartori, I.; Andresen, I. Energy flexibility potential of domestic hot water systems in apartment buildings. *E3S Web Conf.* **2021**, *246*, 11005. [CrossRef]

35. Shen, G.; Lee, Z.E.; Amadeh, A.; Zhang, K.M. A data-driven electric water heater scheduling and control system. *Energy Build.* **2021**, *242*, 110924. [CrossRef]

36. Mor, G.; Cipriano, J.; Grillone, B.; Amblard, F.; Menon, R.P.; Page, J.; Brennenstuhl, M.; Pietruschka, D.; Baumer, R.; Eicker, U. Operation and energy flexibility evaluation of direct load controlled buildings equipped with heat pumps. *Energy Build.* **2021**, *253*, 111484. [CrossRef]

37. Utama, C.; Troitzsch, S.; Thakur, J. Demand-side flexibility and demand-side bidding for flexible loads in air-conditioned buildings. *Appl. Energy* **2021**, *285*, 116418. [CrossRef]

38. Wani, M.; Swain, A.; Ukil, A. Control Strategies for Energy Optimization of HVAC Systems in Small Office Buildings using EnergyPlus^{TM}. In Proceedings of the 2019 IEEE Innovative Smart Grid Technologies—Asia (ISGT Asia), Chengdu, China, 21–24 May 2019; pp. 2698–2703.

39. Peña, M.; Biscarri, F.; Guerrero, J.I.; Monedero, I.; León, C. Rule-based system to detect energy efficiency anomalies in smart buildings, a data mining approach. *Expert Syst. Appl.* **2016**, *56*, 242–255. [CrossRef]

40. Reynders, G.; Diriken, J.; Saelens, D. Generic characterization method for energy flexibility: Applied to structural thermal storage in residential buildings. *Appl. Energy* **2017**, *198*, 192–202. [CrossRef]

41. Rawat, T.; Singh, J.; Sharma, S. Performance Analysis of 400 kWp Rooftop Solar Plant at Swami Keshvanand Institute of Technology, Management & Gramothan, Jaipur using PVsyst. In Proceedings of the 2023 International Conference on Power, Instrumentation, Energy and Control (PIECON), Aligarh, India, 10–12 February 2023; pp. 1–6.

42. Mwammenywa, I.; Petrov, D.; Holle, P.; Hilleringmann, U. LoRa Transceiver for Load Monitoring and Control System in Microgrids. In Proceedings of the 2022 International Conference on Engineering and Emerging Technologies (ICEET), Kuala Lumpur, Malaysia, 27–28 October 2022; pp. 1–5.
43. Kendel, A.; Lazaric, N. The diffusion of smart meters in France. *J. Strat. Manag.* **2015**, *8*, 231–244. [CrossRef]
44. LOI n° 2015-992 Du 17 Août 2015 Relative à la Transition Énergétique Pour la Croissance Verte (1). 2015. Available online: https://www.legifrance.gouv.fr/loda/id/JORFTEXT000031044385/ (accessed on 30 November 2024).
45. Douzane, O.; Promis, G.; Roucoult, J.-M.; Le, A.-D.T.; Langlet, T. Hygrothermal performance of a straw bale building: In situ and laboratory investigations. *J. Build. Eng.* **2016**, *8*, 91–98. [CrossRef]